PROCEEDINGS OF SPIE

SPIEDigitalLibrary.org/conference-proceedings-of-spie

Automatic computational labeling of glomerular textural boundaries

Brandon Ginley, John Tomaszewski, Pinaki Sarder

Brandon Ginley, John E. Tomaszewski, Pinaki Sarder, "Automatic computational labeling of glomerular textural boundaries," Proc. SPIE 10140, Medical Imaging 2017: Digital Pathology, 101400G (1 March 2017); doi: 10.1117/12.2254517

SPIE.

Event: SPIE Medical Imaging, 2017, Orlando, Florida, United States

Automatic computational labeling of glomerular textural boundaries

Brandon Ginley[1], John E. Tomaszewski[1,2], and Pinaki Sarder[1,3,4,*]

Departments of [1]Pathology and Anatomical Sciences, [2]Biomedical Informatics, [3]Biomedical Engineering, and [4]Biostatistics

University at Buffalo – The State University of New York,
207 Farber Hall, 3435 Main Street
Buffalo, NY 14214, USA

[*]Address all correspondence to: Pinaki Sarder
Tel: 716-829-2265; E-mail: pinakisa@buffalo.edu

ABSTRACT

The glomerulus, a specialized bundle of capillaries, is the blood filtering unit of the kidney. Each human kidney contains about 1 million glomeruli. Structural damages in the glomerular micro-compartments give rise to several renal conditions; most severe of which is proteinuria, where excessive blood proteins flow freely to the urine. The sole way to confirm glomerular structural damage in renal pathology is by examining histopathological or immunofluorescence stained needle biopsies under a light microscope. However, this method is extremely tedious and time consuming, and requires manual scoring on the number and volume of structures. Computational quantification of equivalent features promises to greatly ease this manual burden. The largest obstacle to computational quantification of renal tissue is the ability to recognize complex glomerular textural boundaries automatically. Here we present a computational pipeline to accurately identify glomerular boundaries with high precision and accuracy. The computational pipeline employs an integrated approach composed of Gabor filtering, Gaussian blurring, statistical F-testing, and distance transform, and performs significantly better than standard Gabor based textural segmentation method. Our integrated approach provides mean accuracy/precision of 0.89/0.97 on $n = 200$ Hematoxylin and Eosin (H&E) glomerulus images, and mean 0.88/0.94 accuracy/precision on $n = 200$ Periodic Acid Schiff (PAS) glomerulus images. Respective accuracy/precision of the Gabor filter bank based method is 0.83/0.84 for H&E and 0.78/0.8 for PAS. Our method will simplify computational partitioning of glomerular micro-compartments hidden within dense textural boundaries. Automatic quantification of glomeruli will streamline structural analysis in clinic, and can help realize real time diagnoses and interventions.

Keywords: Glomerulus, Gabor filter, image segmentation, F-test, distance transform, histology.

1. INTRODUCTION

The kidney is the organ of the body which filters blood to produce urine. The essential regulatory role of maintaining electrolyte and pH concentration is performed by the nephron, and each nephron is spearheaded by a glomerulus. Each human kidney contains 900,000 to 1 million nephrons[1]. The glomerulus is approximately spherical with diameter 200 µm, and is an entangled bundle of capillaries surrounded by multiple specialized cell lines which each have specific tasks to maintain in filtering blood[2]. Structural damage to one or more of these specialized cells reduces the ability of the kidney to filter and leads to a multitude of renal diseases, which often progressively intensify until end stage renal disease or death[3, 4]. Medicare reports that each year there are approximately 525K U.S. patients with end stage kidney failure, the care of whom costs the healthcare system over $24 billion[5]. The proteinuric condition of diabetic nephropathy alone causes ESRD for >225K U.S. patients accounting for >$19K in Medicare cost per patient[6]. Proteinuria is common in renal disease, and refers to the excess spilling of blood serum proteins to the urine; this level of protein is a widely used marker to track renal disease progression[7]. However, it has been shown there is only a weak association between proteinuria and glomerular damage[3, 8].

Therefore, when renal malfunction is suspected, diagnosing the source and identifying a proper therapy requires manual inspection of the structural conformation of multiple glomeruli under light microscopy. While this approach is the gold standard in clinic, it is time consuming, tedious, and semi-quantitative. These limitations are due to the extreme heterogeneity inherent in renal tissue, an obstacle which has also hindered robust computational quantification methods

Medical Imaging 2017: Digital Pathology, edited by Metin N. Gurcan, John E. Tomaszewski, Proc. of SPIE Vol. 10140, 101400G · © 2017 SPIE · CCC code: 1605-7422/17/$18 · doi: 10.1117/12.2254517

from being developed in the past. There is an immediate need for a computational scheme that can accurately and precisely locate and quantify glomerular structures. Automatic, concrete numerical measurements taken digitally would provide a much higher degree of diagnostic information in a smaller amount of time, thereby improving diagnosis of renal disease, improving oversight on therapeutic efficacy, and reducing healthcare burden.

As a first step towards this goal, we have developed an unsupervised method capable of precisely defining the boundary of the glomerulus in renal histology images stained with Hematoxylin and Eosin and Periodic Acid-Schiff. Prior glomerular segmentation methods are both supervised and unsupervised, using edge detection and patching with genetic algorithms[9, 10], curve fitting[11], or a combination of Icy[12] and Cytomine[13, 14]. However, these methods have drawbacks that limit translational potential to the clinic. Supervised methods require large training sets to achieve high performance, the time and data of which may be unavailable in the real clinic. Edge detection methods are limited by the prominence of the Bowman's space and capsule, which may or may not be present in disease samples. On the contrary, Gabor filtering[15] does not require specific training and does not directly rely on the prominence of the Bowman's space and capsule. To the extent of our knowledge, there are no past unsupervised works which approach the robustness, precision, and accuracy offered by our method.

Our method first discriminates a textural boundary mask between the glomerulus and surroundings using Gabor filtering. Subsequently, the pixel intensities contained within the region defined by the Gabor mask are F-tested[16] for similar variance in a local window. This results in a second mask, and the distance transform[22] of both masks is taken. A third image is defined as a weighting map, which has highest weight in the center of the image and decreases uniformly to zero at the image edges. Thresholding the average of all three images yields the final glomerular boundary, which shows improved precision and accuracy over Gabor filtering alone which we reported in past work[17, 18].

By conducting glomerular boundary segmentation, we have paved the path to expedite the analysis of standard intra-glomerular micro-compartments, which promise high clinical impact if computationally quantified. Clinically relevant glomerular micro-compartments are glomerular volume, podocyte effacement and death, changes in mesangial cellularity and matrix volume, and lumen content[19]. These benchmark indicators are already clinically known to provide informative power on the source and trajectory of renal disease, but cannot be quantified if glomerular regions are not identified from tubular regions. The envisioned pipeline can be part of a semi-supervised digital pathology workflow, where pathologists accept or reject proper segmentations to speed data collection and accurate feature extraction. This approach will provide a faster statistical sampling in clinical pathology than the current practice, and will ensure accuracy in diagnosis. The ultimate aim of our approach is to further facilitate development of digital protocols which quantify glomerular features and motivate the shift of renal pathology to a computational era.

2. RESULTS

Fig. 1 shows the processing pipeline proposed to segment accurate glomerular boundaries. Fig. 1A is an example of an individual rat glomerulus stained with Hematoxylin and Eosin (H&E). Each image is first converted to a grayscale intensity image, shown in Fig. 1B. This image is then blurred with a Gaussian function having a deviation with values selected discretely for each stain type, see Fig. 1C. Gabor textural filtering[20] generates a primary mask identifying glomerular regions. The first principal component[21] of the Gabor filter bank delineating the glomerular texture as a heatmap is shown in Fig. 1D, and the corresponding glomerular regions, clustered by *K*-means, in Fig. 1E. Statistical F-testing[16] the entire image in Fig. 1A for similarity with regions identified in Fig. 1E yields a secondary mask. This mask is morphologically processed further to remove small erroneous segments. Distance transform is applied to both the Gabor output and the F-test output, the intensity heatmaps of which are shown in Figs. 1H and 1I, respectively. A third mask is generated by assigning each pixel to be 0.75 of its Euclidean distance from the center. This mask is then inverted to yield high intensity in central regions, and low intensity on outer regions, see Fig. 1J. Averaging this mask with distance transformed masks shown in Figs. 1H and 1I smoothens imperfections between both the Gabor and F-testing methods, and deemphasizes structures outside image boundaries, see Fig. 1K. Fixed value thresholding of the intensity heatmap shown in Fig. 1K yields the final glomerular boundary, see Fig. 1L.

Our proposed integrated computational pipeline is able to accurately localize glomerular boundaries with mean accuracy/precision of 0.89/0.97 over $n = 200$ H&E stained individual glomerulus images, and mean accuracy/precision of 0.88/0.94 over $n = 200$ Periodic Acid Schiff (PAS) glomerulus images. This is an improvement over Gabor filter bank based textural segmentation method[17], where H&E stained glomeruli scored 0.83/0.84 accuracy/precision, and PAS stained glomeruli scored 0.78/0.80 accuracy/precision. Fig. 2 summarizes these results. Figs. 2A and 2B show typical H&E

segmentation of glomeruli using the improved method, and Figs. 2C and 2D show typical PAS segmentation of glomeruli. Fig. 2E shows a scatterplot of accuracy vs precision for 200 H&E images, where the improved method is marked in red, and the method with Gabor only is marked in black. The same information is depicted for PAS images in Fig. 2F. Note that while the literature in computational informatics is typically familiar with either a precision/recall based performance analysis (preferred approach of a computer scientist) or sensitivity/specificity based performance analysis (preferred approach of a statistician), we have chosen precision and accuracy. In the case of glomerular boundary segmentation, due to heterogeneity, it is not possible for a manual annotator to perfectly assign each pixel close to the boundary into the correct class. Rather, human visual annotation attempts to generalize the segmentation boundary and approximate the error tradeoff between foreground and background. Thus, for maximum performance, it is not necessarily advantageous to optimize segmentation of the background or foreground, but rather try to closely mimic the error trade-off approximated boundary by human annotation. Accuracy is thus ideal for this comparison, as the true positive and true negative classifications are given a higher weight than false negative and false positive classifications, showing how much of the input image was correctly classified and de-emphasizing small mistakes close to the boundary. Precision is a complementary performance metric to accuracy, demonstrating strictly how much of the glomerulus was correctly labeled.

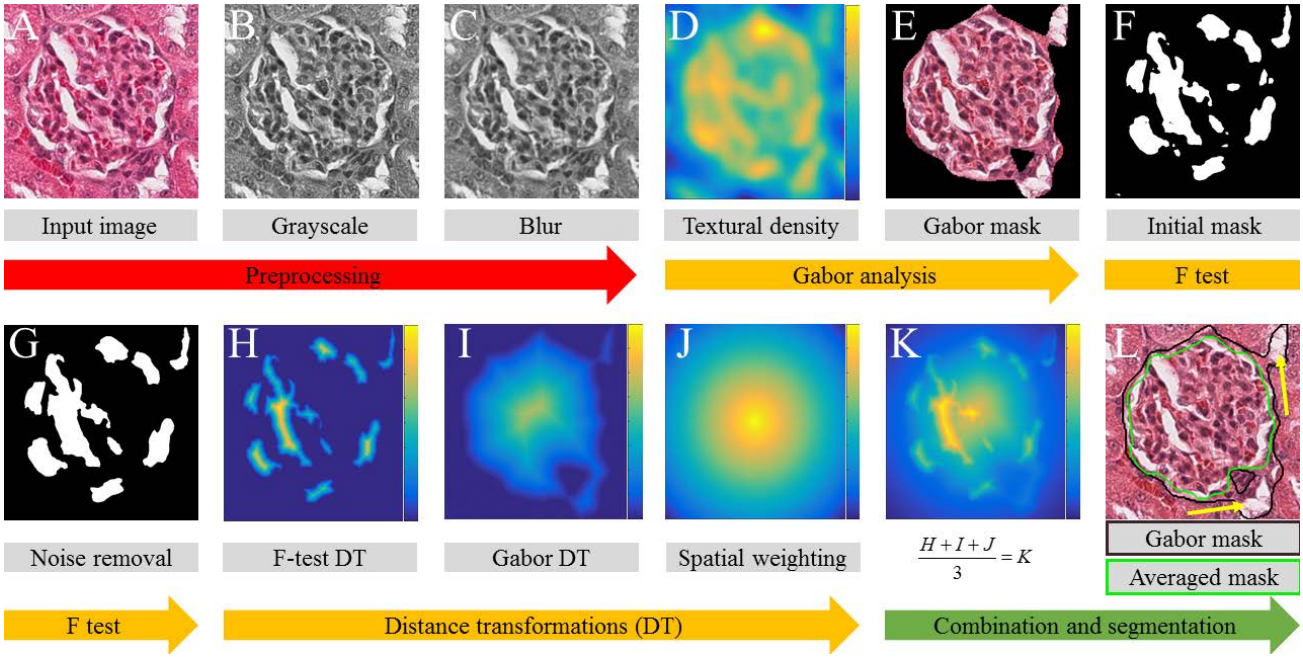

Fig. 1. Demonstration of the image processing pipeline used to derive accurate glomerular boundaries[17, 18]. (A) Hematoxylin and eosin stained glomerular tissue image. (B) Grayscale version of the image shown in A. (C) Gaussian blurred image of B. (D) Intensity image of the first principal component of the Gabor filter bank outputs using as input the image shown in C. (E) *K*-means clustering is used to find final Gabor boundary. (F) F-testing examines the entire image for similarity with E, and outputs 0 or 1 for each pixel. (G) Morphological noise removal for the image in F. (H-I) Distance transformed images of the respective binary masks obtained from F-testing and Gabor textural segmentation. (J) Intensity image of a spatial weighting map obtained from A. (K) Heatmap of an average of intensity images in H-J. (L) Final segmentation after thresholding shown using green. The segmentation obtained from initial Gabor based method (see E) is shown using black. The green boundary depicts improved detection of glomerulus. Yellow arrows indicate tubular lumen close to the glomerular boundary, the most common source of error under this method.

3. METHODS

3.1. Tissue slicing and preparation

Intact kidney tissues from normal healthy untreated rats were collected from Dr. Tracey Ignatowski (Pathology and Anatomical Sciences, University at Buffalo) and sacrificed under their protocol. Tissues were formalin fixed, embedded in paraffin blocks, sliced at 5 µm and stained with H&E and PAS. Imaging was conducted using a whole slide bright field microscope (Aperio, Leica, Buffalo Grove, IL) using a 40× objective with 0.75 NA. Pixel resolution is 0.25 µm, and an average rat glomerulus diameter was measured to be 105 ± 11 µm. The computational method proposed here has been

constructed around this imaging configuration, and the parameter values may change proportionally for other imaging conditions.

3.2. Ground-truth segmentation

Ground-truth segmentation for the glomerular boundary was obtained by manual hand segmentation of the glomerular boundary by the author Mr. Brandon Ginley, who is a PhD student, under the supervision of the co-author Dr. John Tomaszewski, who is a renal pathologist.

3.3. Gabor textural segmentation

Our group has extensively reviewed texture segmentation using Gabor filter bank in a recent work[18].

3.4. F-test based segmentation

To perform F-test segmentation[16], first the measurements denoted by $z_1, z_2, z_3, ..., z_N$ with variance σ_z^2 are taken from the intra-glomerular region identified from Gabor output. Next, the measurements $w_1, w_2, w_3, ..., w_M$ with variance σ_w^2 are taken from a local window that is iteratively centered on every pixel in the image. The testing problem is defined by, $H_0 : \sigma_z^2 = \sigma_w^2$ vs $H_a : \sigma_z^2 > \sigma_w^2$, where H_0 is the null hypothesis and H_a is the alternative hypothesis. The test statistic is given by, $F = \widehat{\sigma_z^2} / \widehat{\sigma_w^2}$, which is F-distributed with $N-1$ and $M-1$ degrees of freedom. The null hypothesis is rejected, when $F > F_{\alpha, N-1, M-1}$, where $F_{\alpha, N-1, M-1}$ is the critical value of the F-distribution with $N-1$ and $M-1$ degrees of freedom and for a significance level α. Each pixel is then assigned 0 for a rejected test, and 1 for a passing test, creating a binary segmentation mask.

3.5. Distance transforms

Distance transforms[22] operate on binary images, reassigning each foreground pixel with its distance to the closest background pixel. We apply this transformation to both the Gabor output mask, as well as the F-test mask. We apply a slightly modified form of the distance transform to generate a third mask, where each pixel is assigned to be 0.75 time of its Euclidean distance to the center. This mask is then inverted to transform low valued center pixels to high value.

3.6. Final segmentation

Averaging all three distance transformed masks, and fixed value thresholding, yields the final glomerular boundary.

4. DISCUSSION

We have shown for the first time automatic and robust segmentation of complex glomerular textural boundary in renal histopathology. Moreover, statistical F-testing has not been used for image segmentation in the past. Gabor textural segmentation is known in the literature to be an effective tool for discriminating textural boundaries, as we discussed previously[17]. We demonstrate here for the first time that the performance of the Gabor textural segmentation can be boosted by incorporating information from statistical F-testing to delineate textural regions in histopathological images. F-testing helps to improve performance of the method because the distribution in intensity of pixel values within glomerular regions is statistically distinct from extra-glomerular regions. Distance transform helps to improve the performance of the method by weighting pixels to have higher influence if they exist far from the boundary of identified objects. This assigns a pseudo-likelihood of a pixel belonging to a specified object. This is useful because erroneous objects are identified in both the Gabor and F-test step, but both modalities show different erroneous objects. After weighting and averaging, the erroneous communities of pixels which are not significantly large or are not represented in all sources are attenuated. The third mask, a spatial weighting mask, shown in Fig. 1J, serves to bind the F-test mask and Gabor mask together in places where there is an inconsistency in the boundary, and also helps to emphasize the elliptical nature of glomeruli.

The biggest challenge to accurate segmentation using this method is the presence of tubular lumen close to the glomerular boundary. An example of tubular lumen close to the glomerular boundary is shown in Fig. 1L with yellow arrows. It is exceedingly difficult to differentiate between the two lumen types because they exhibit similar pixel intensity and variance, and are only marginally morphologically distinct. To overcome this obstacle, we will expand the method with an additional step, where we measure the average change in the convex hull of the final segmentation, as each individual lumen object

is iteratively removed separately from the segmentation. We expect that any single glomerular lumen will have a minimal influence on the boundary if removed, because it is contained within the boundary. On the other hand, because tubular lumen exists outside the boundary of the glomerulus, we expect it will change the average convex hull shape by a much greater deviation. We predict this will allow accurate identification and removal of tubular lumen with minimal removal of glomerular lumen and Bowman's space.

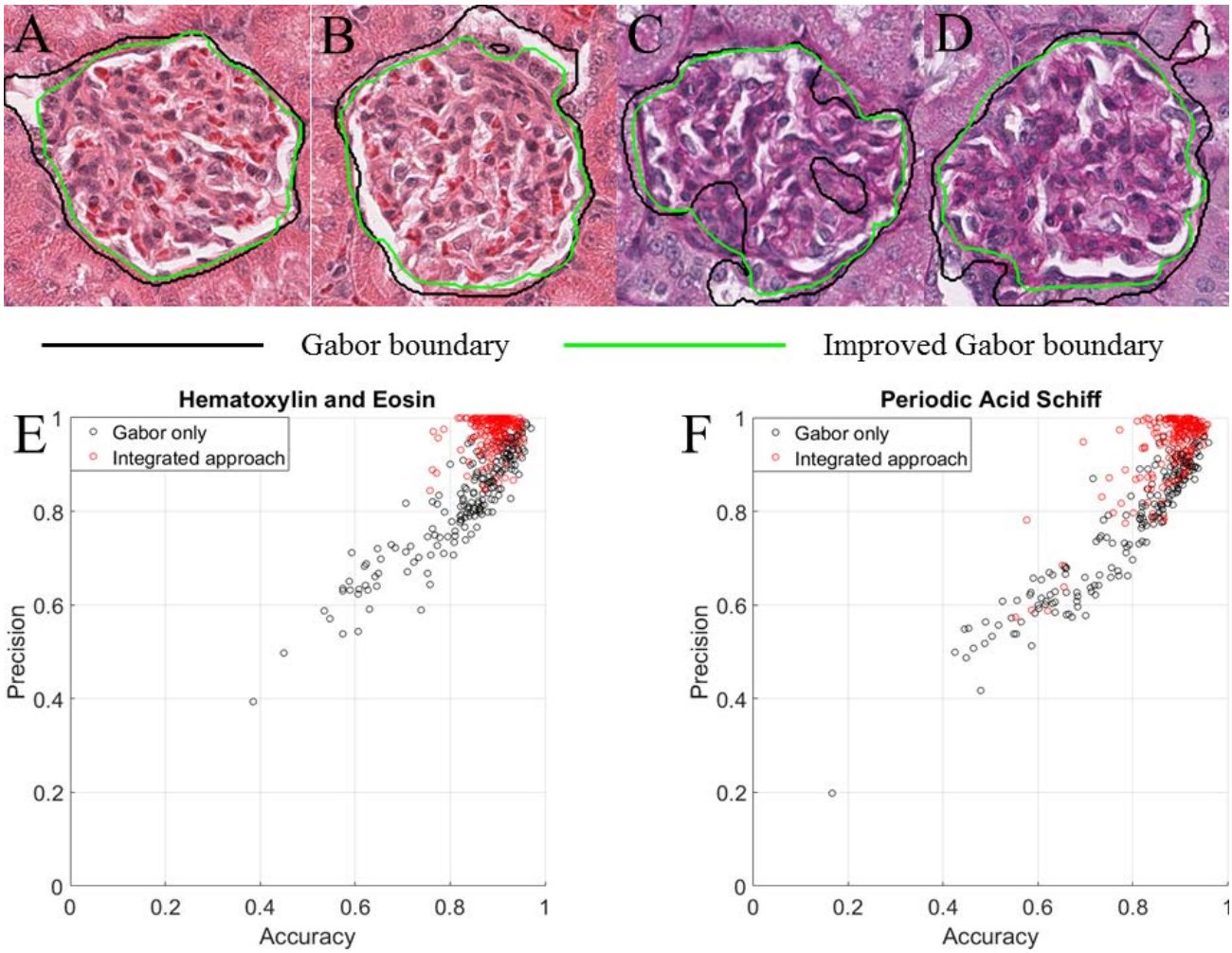

Fig. 2. Typical segmentation performance of the proposed segmentation pipeline. (A-B) Segmentation of Hematoxylin and eosin (H&E) stained images using Gabor and the improved method. (C-D) Segmentation of Periodic Acid Schiff (PAS) stained images. (E) Performance of 200 H&E images with the integrated pipeline (red) compared to the Gabor filter bank based method (black). (F) Performance of 200 PAS images in the same manner.

5. CONCLUSION

This study shows for the first time that automated textural segmentation of renal glomeruli can be improved with statistical tools. Automated renal histopathology is the introduction of the answer to the current clinical obstacles in renal histopathology. Our first steps towards automated quantification of renal tissue prefaces rapid access to global structural information by clinical pathologists. In addition to the positive results of this study, the parameters of this method can still be further optimized to achieve higher performances. Future development on this method will involve complete optimization of the parameters in this method, and extension to several more common histological stains. Eventually we will also explore more cutting edge techniques, such as convolutional neural networks[23] or rolling guidance filters[24], and compare which filtering routines provide the optimal framework to maximize performance and efficiency of textural

filtering in renal applications[25, 26]. We hope our work aids further clinical and academic research into the numerical quantification of renal disease, and boosts the translational potential of digital renal pathology.

ACKNOWLEDGMENTS

This project was supported by the faculty start-up funds from the Pathology & Anatomical Sciences Department, Jacobs School of Medicine and Biomedical Sciences, University at Buffalo. We thank the histology core facility personnel, Ms. Annette Featherstone and Ms. Donna Carapetyan (Pathology & Anatomical Sciences, University at Buffalo), for performing histopathological slicing and staining of tissues.

REFERENCES

[1] Bertram, J. F., Douglas-Denton, R. N., Diouf, B. *et al.*, "Human nephron number: implications for health and disease," Pediatr Nephrol, 26(9), 1529-33 (2011).
[2] Hall, T. J., Insana, M. F., Harrison, L. A. *et al.*, "Ultrasonic measurement of glomerular diameters in normal adult humans," Ultrasound Med Biol, 22(8), 987-97 (1996).
[3] Lopez-Novoa, J. M., Rodriguez-Pena, A. B., Ortiz, A. *et al.*, "Etiopathology of chronic tubular, glomerular and renovascular nephropathies: clinical implications," J Transl Med, 9, 13 (2011).
[4] Gross, J. L., de Azevedo, M. J., Silveiro, S. P. *et al.*, "Diabetic nephropathy: diagnosis, prevention, and treatment," Diabetes Care, 28(1), 164-76 (2005).
[5] Chronic kidney disease and kidney failure Available from: http://report.nih.gov/nIHfactsheets/ViewFactSheet.aspx?csid=34&key=C
[6] National Association of Chronic Disease Directors Available from: http://www.chronicdisease.org/
[7] Gorriz, J. L. and Martinez-Castelao, A., "Proteinuria: detection and role in native renal disease progression," Transplant Rev (Orlando), 26(1), 3-13 (2012).
[8] Kidney biopsy. Available from: https://www.niddk.nih.gov/health-information/health-topics/diagnostic-tests/kidney-biopsy/Pages/kidney-biopsy.aspx
[9] Ma, J. X., Zhang, J. and Hu, J. L., "Glomerulus Extraction by Using Genetic Algorithm for Edge Patching," 2009 Ieee Congress on Evolutionary Computation, Vols 1-5, 2474-2479 (2009).
[10] Zhang, J., Hu, J. L. and Zhu, H., "Contour Extraction of Glomeruli by Using Genetic Algorithm for Edge Patching," Ieej Transactions on Electrical and Electronic Engineering, 6(3), 229-235 (2011).
[11] Zhang, J. and Hu, J. L., "Glomerulus Extraction by Optimizing the Fitting Curve," Proceedings of the 2008 International Symposium on Computational Intelligence and Design, Vol 2, 169-172 (2008).
[12] Icy Available from: http://icy.bioimageanalysis.org/
[13] Cytomine Available from: http://www.cytomine.be/
[14] Maree, R., Dallongeville, S., Olivo-Marin, J. C. *et al.*, "An Approach for Detection of Glomeruli in Multisite Digital Pathology," 2016 Ieee 13th International Symposium on Biomedical Imaging (Isbi), 1033-1036 (2016).
[15] Jain, A. K. and Farrokhnia, F., "Unsupervised Texture Segmentation Using Gabor Filters," Pattern Recognition, 24(12), 1167-1186 (1991).
[16] Hogg, R. V., Craig, A. and McKean, J. W., [Introduction to Mathematical Statistics], Prentice Hall, Upper Saddle River, New Jersey, 1-692 (2004).
[17] Sarder, P., Ginley, B. and Tomaszewski, J. E., "Automated renal histopathology: Digital extraction and quantification of renal pathology," Proceedings of SPIE (SPIE Medical Imaging 2016: Digital Pathology), 9791, 97910F: 1-12 (2016).
[18] Ginley, B., Tomaszewski, J., Yacoub, Y. *et al.*, "Unsupervised labeling of glomerular boundaries using Gabor filters and statistical testing in renal histology," Journal of Medical Imaging, (to appear).
[19] D'Amico, G. and Bazzi, C., "Pathophysiology of proteinuria," Kidney Int, 63(3), 809-25 (2003).
[20] Jain, A. and Farrokhnia, F., "Unsupervised texture segmentation using Gabor filters," Pattern Recognition, 24(12), 1167-1186 (1991).
[21] Gonzalez, R. C. and Woods, R. E., [Digital Image Processing], Prentice Hall, 1-976 (2007).
[22] Maurer, C., "A Linear Time Algorithm for Computing Exact Euclidean Distance Transforms of Binary Images in Arbitrary Dimensions," IEEE Trans Pattern Analysis and Machine Intelligence, 25(2), 265-270 (2003).
[23] Caffe: Deep Learning Framework Available from: http://caffe.berkeleyvision.org/
[24] Zhang, Q., Shen, X., Xu, L. *et al.*, [Rolling Guidance Filter] Springer International Publishing, Cham(2014).
[25] LeCun, Y., Bengio, Y. and Hinton, G., "Deep learning," Nature, 521(7553), 436-44 (2015).
[26] Zhang, Q., Shen, X. Y., Xu, L. *et al.*, "Rolling Guidance Filter," Computer Vision - Eccv 2014, Pt Iii, 8691, 815-830 (2014).